

Pressure-induced superconductivity in the orthorhombic Kondo compound CePtSi₂

Tomohito Nakano,¹ Masashi Ohashi,^{1,2} Gendo Oomi,¹ Kazuyuki Matsubayashi,³ and Yoshiya Uwatoko³

¹Department of Physics, Kyushu University, Hakozaki 6-10-1, Fukuoka 810-8581, Japan

²Natural Science and Technology, Kanazawa University, Kakuma-machi, Kanazawa, Ishikawa 920-1192, Japan

³Institute for Solid State Physics, University of Tokyo, Kashiwanoha 5-1-5, Kashiwa, Chiba 277-8581, Japan

(Received 1 July 2008; revised manuscript received 15 December 2008; published 28 May 2009)

We have discovered a member of superconductivity induced by hydrostatic pressure in an antiferromagnetic (AF) concentrated Kondo compound CePtSi₂ by measuring the resistivity and magnetoresistance. The AF transition temperature T_N of 1.8 K at ambient pressure is suppressed by pressure and disappears around 1.2 GPa. Above 1.4 GPa, a superconducting phase appears between 1.4 and 2.4 GPa, with the maximum T_c of 0.14 K at 1.7 GPa. The upper critical field of the superconductivity is evaluated to be 0.7 T, which is clearly larger than that of the Pauli limit predicted by the BCS theory.

DOI: 10.1103/PhysRevB.79.172507

PACS number(s): 74.70.Tx, 71.27.+a

The discovery and understanding of these phenomena in condensed matters give rise to the most important progress in this research field. A typical example is the so-called quantum phase transition, which is often accompanied by a new quantum phase, such as superconductivity¹⁻¹⁰ and non-Fermi liquid¹¹⁻¹⁷ around the quantum critical point (QCP). In strongly correlated electron systems, various quantum phase transitions have been reported to be induced by controlling interactions of the spin, orbital, electron, phonon, and so on using external forces. In the concentrated Kondo Ce compounds, a competition between the Ruderman-Kittel-Kasuya-Yosida (RKKY) interaction and the Kondo effect can be tuned by changing hybridization of 4*f* orbital and conduction band. This is well displayed in the Doniach phase diagram¹⁸ as a function of $J_{cf}D(E_F)$, where J_{cf} is the exchange interaction between *f* and conduction electrons, and $D(E_F)$ is the density of states at the Fermi energy E_F . Magnetic-nonmagnetic quantum phase transition occurs when the Kondo effect overcomes RKKY interaction by changing magnetic field, chemical substitution, or pressure. In such sense, the concentrated Kondo compound CePtSi₂ is a possible candidate which exhibits a new quantum phase with an application of pressure, as will be mentioned in the following.

CePtSi₂ has a CeNiGe₂-type orthorhombic layered structure (space group *Cmcm*), where the Ce and Pt-Si layers are stacked alternatively along the *b* axis, with lattice constants $a=4.288$, $b=16.718$, and $c=4.238$ Å,¹⁹ as shown in Fig. 1. The electronic specific-heat coefficient γ of the paramagnetic state is 600 mJ/mol K² (Ref. 20) and the characteristic Kondo temperature T_K evaluated from the specific heat, resistivity, and magnetization measurements is 3 K.¹⁹ An AF transition occurs around $T_N=2$ K, which was associated with a jump in specific heat¹⁹⁻²² and an upward bend in thermal expansion.²³ It has been found that pressure suppresses the AF phase and the QCP is predicted to exist around 1.1 GPa.²² Non-Fermi-liquid behavior was observed around 1.1 GPa in which the resistivity shows linear T dependence in the low-temperature region (~ 2 K).²⁴ Conventional Fermi-liquid behavior, which is characterized by T^2 dependence in the low-temperature resistivity, recovers above 2 GPa.²⁴ In this study, we attempted to measure the resistivity of CePtSi₂ under high pressure in the low-

temperature region and found a superconductivity accompanied with disappearance AF phase by application of pressure.

A polycrystalline sample of CePtSi₂ was synthesized by arc-melting stoichiometric amounts of Ce (3N), Pt (4N), and Si (5N) in an Ar atmosphere. The obtained button was remelted several times to ensure homogeneity and annealed at 1000 °C in an evacuated quartz tube for three weeks. The result of electron probe microanalysis (EPMA) is shown in Table I. It shows no dispersion in the concentration at the sample position indicating that homogenous chemical composition is close to that of stoichiometric CePtSi₂. Almost peaks in the powder x-ray diffraction pattern were indexed by CeNiGe₂-type structure except some unidentified weak peaks associated with interplanar spacing $d=3.615$, 3.180, 2.600, and 2.507 Å. The maximum peak intensity of the impurity phases with $d=2.600$ Å is almost consistent with (112) and (103) reflection of CePt₂Si₂ (CaBe₂Ge₂-type)²⁵ and CePtSi₃ (BaNiSn₃-type),²⁶ respectively, and is as much as 10% of that for the matrix of CePtSi₂ indicating about sev-

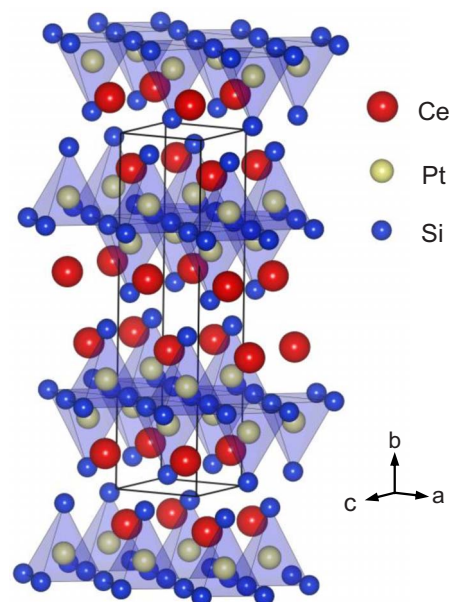


FIG. 1. (Color online) Crystal structure of orthorhombic CePtSi₂.

TABLE I. Concentrations at some positions in the sample measured by EPMA.

Position	Concentration (at.%)		
	Ce	Pt	Si
1	24.91	25.71	49.38
2	24.81	25.83	49.36
3	24.95	25.49	49.62
Ave.	24.89	25.68	49.45

eral percents impurity phases. The sample was cut by a spark cutter into a size of $0.5 \times 1 \times 1$ mm³. The resistivity was measured by a standard ac four-probe method using an LR700 resistance bridge with a dilution refrigerator down to 50 mK under hydrostatic pressure up to 2.6 GPa. Pressure was generated using a NiCrAl-CuBe alloy hybrid piston-cylinder cell.²⁷ Daphne-oil 7373 was used as the pressure transmitting medium. A magnetic field up to 0.7 T was applied parallel to the current direction, using a 20 T superconducting magnet. The ac susceptibility was measured using a mutual-inductance method with a modulation frequency and field is 1 kHz and 0.02 Oe, respectively. Hydrostatic pressure was generated with the same setting as in the resistivity measurement.

Figure 2(a) displays the resistivity ρ of the polycrystalline CePtSi₂ sample at various pressures. The excitation current was decreased stepwise with decreasing temperature, and is the order of 100 μ A for the lowest measured temperature. At ambient pressure, ρ increases with decreasing temperature from 300 K and shows two maxima at 23 K ($=T_2$) and 7 K ($=T_1$). These two maxima are well-known characteristic fea-

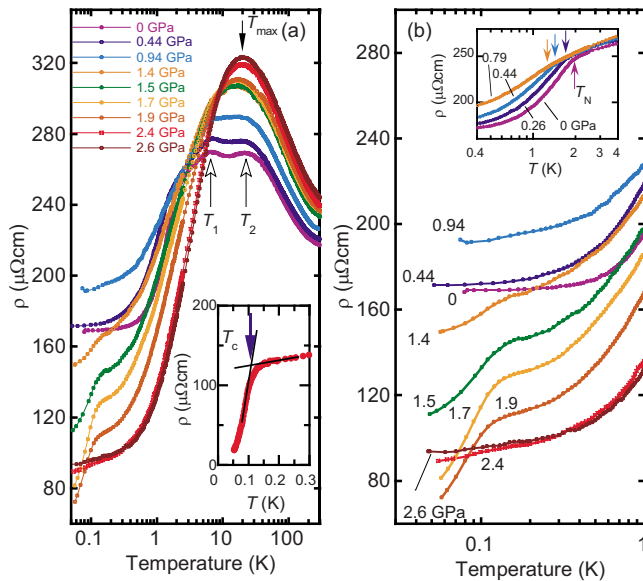


FIG. 2. (Color online) (a) Temperature dependence of the resistivity of CePtSi₂ under hydrostatic pressure. Inset: Details of resistivity around T_c at 1.7 GPa with an excitation current. (b) Resistivity of CePtSi₂ for an extended low-temperature region. Inset: Details of resistivity around T_N under pressures up to 0.79 GPa.

tures of Ce-based Kondo compounds, typical of interplay between the Kondo effect and crystal electric field (CEF) splitting. As the temperature is decreased further below 7 K, ρ decreases and shows a sharper decrease due to the AF transition. We defined the intersection of two linear lines extrapolated from just above and below the inflection point as T_N , which was evaluated to be 1.8 K at ambient pressure. Below T_N , ρ is proportional to T^2 indicating conventional Fermi-liquid-like behavior. These are in fairly good agreement with previous measurements.²⁴

In particular, the pressure clearly changes the overall features in $\rho(T)$, as shown in Figs. 2(a) and 2(b). The effect of pressure on low-temperature resistivity is drastic. T_N decreases with increasing pressure up to 0.79 GPa, as shown in the inset of Fig. 2(b). The pressure dependence of T_N , dT_N/dP , is found to be -1 K/GPa, which is roughly consistent with the result of previous specific-heat measurement.²² The anomaly due to the AF transition disappears above 0.9 GPa showing a deviation from the linear-pressure dependence of T_N . Instead of the AF anomaly, another abrupt resistivity drop appears around 0.15 K above $P_{c1}=1.4$ GPa suggesting a superconducting transition. This resistivity drop develops with increasing pressure up to 1.7 GPa and is observed up to $P_{c2}=2.1$ GPa. We also measured the ρ with a low electric current of 10 μ A at 1.7 GPa, as shown in the inset of Fig. 2(a). ρ at 1.7 GPa with 10 μ A current drops more sharply than that with 100 μ A and is expected to be close to zero below 50 mK. Such current dependence of ρ is considered to be due to the self-heating by an excitation current, which that is a typical feature of superconductivity. We defined the crosspoint between two extrapolated lines just above and below the onset of the resistivity drop as the superconducting transition temperature T_c , which was evaluated to be 0.14 K at 1.7 GPa. The values of T_c and T_N are shown in Fig. 3(a) as a function of pressure.

In addition, we measured the magnetoresistance of CePtSi₂ at 1.7 GPa. Figure 4 shows the low-temperature resistivity with magnetic fields (H) up to 0.7 T, parallel to the excitation current direction. The resistivity drop due to the superconducting transition is suppressed by magnetic field and disappears above $H=0.7$ T. This is a further direct evidence of the superconducting transition in CePtSi₂. Field dependence of T_c is displayed in the inset (a) of Fig. 4. The upper critical field H_{c2} is found to be 0.7 T at 1.7 GPa. We evaluated H_{c2}/T_c to be 5 (T/K), which is clearly larger than the Pauli limit of 1.86 (T/K) predicted by the BCS theory.

The ac susceptibility χ_{ac} for the same sample at 1.8 GPa is shown in the inset (b) of Fig. 4. χ_{ac} drops below $T_c \sim 0.12$ K, which is consistent with that evaluated from the resistivity measurement. This is also a clear evidence of superconducting ordering. This drop and T_c are suppressed by application of a magnetic field and disappear above 0.3 T as shown in the inset (b) of Fig. 4. These behaviors are consistent with the results of the resistivity measurement. We evaluated the superconducting volume fraction of CePtSi₂ at 0.04 K to be about 30%, indicating that the superconductivity of CePtSi₂ should be a bulk phenomenon. Here, the difference between $\chi_{ac}(H=0$ T) and the linear extrapolation of $\chi_{ac}(H=0.3$ T) at 0.04 K is evaluated as the variation in the ac susceptibility $\Delta\chi_{ac}$ due to the superconducting ordering,

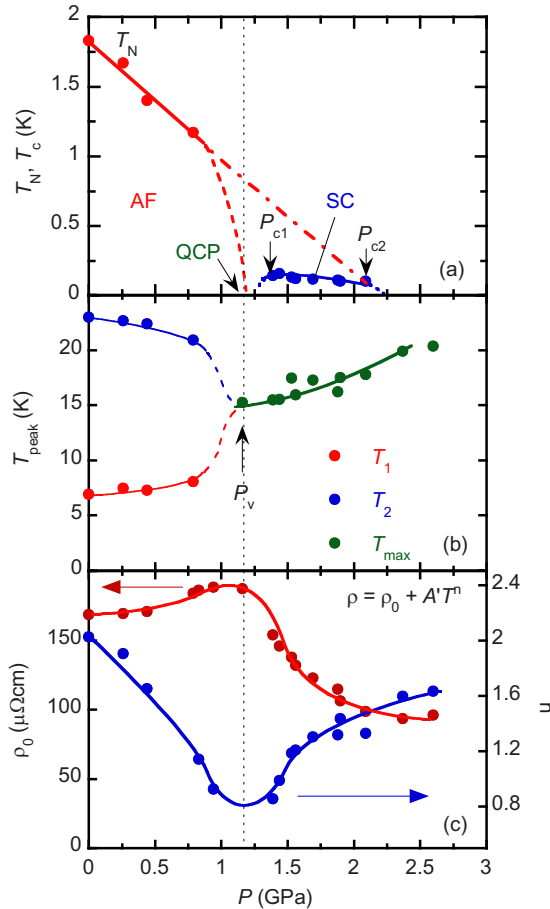


FIG. 3. (Color online) (a) Phase diagram of CePtSi₂ under pressure. The dashed line is an expectation of pressure dependence of T_N . The dash-dotted line is a linear extrapolation of the pressure dependence of T_N based on the magnetic interactions model for a two-dimensional AF. Pressure dependence of (b) T_1 , T_2 , and T_{max} , (c) ρ_0 and n , respectively. The lines are guides for the eyes.

as shown in the inset (b) of Fig. 4. This value is clearly larger than the ratio of the impurity phase(s) evaluated from the x-ray measurements. Thus, we conclude that the pressure-induced superconductivity of CePtSi₂ is an intrinsic phenomenon. On the other hand, zero resistivity was not observed despite the presence of bulk superconductivity indicating that current dependence of the resistivity below T_c is due to self-heating by an excitation current rather than the intrinsic current dependence of superconductivity. Indeed, the resistivity below T_c is close to zero with decreasing excitation current as shown in inset of Fig. 2(a).

The pressure dependence of the high-temperature resistivity is also interesting. As shown in Fig. 3(b), T_1 increases with increasing pressure up to 0.9 GPa, whereas T_2 decreases. The pressure dependence of T_1 and T_2 was reported for several Ce-based Kondo compounds, such as CeCu₂Si₂,²⁸ CeCu₂Ge₂,²⁹ and CeAl₂ (Ref. 30) in which T_1 and T_2 are associated with modified Kondo temperatures owing to the CEF splitting. It should be noted that T_1 and T_2 merge into a single maximum (at T_{max}) above 1.15 GPa. We defined the pressure as P_V , which is nearly the same as P_{c1} . In general, the Kondo effect is enhanced by applying pressure because

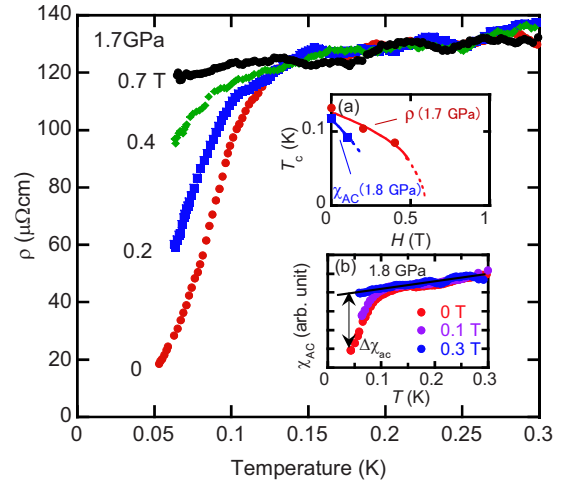


FIG. 4. (Color online) Resistivity of CePtSi₂ with a magnetic field up to 0.7 T under 1.7 GPa. Inset: (a) Magnetic-field dependence of T_c at 1.7 GPa and 1.8 GPa evaluated from resistivity and ac susceptibility, respectively. Inset: (b) Temperature dependence of χ_{ac} for CePtSi₂ under 1.8 GPa in various magnetic fields.

of the enhanced hybridization between the conduction d and magnetic f electrons due to the decrease in lattice constants and consequent overlap of CEF-split levels. Thus, the increases in T_1 and T_{max} indicate an increase in T_K . On the other hand, the decrease in T_2 may be attributed to CEF rather than the variation in Kondo temperature.

Low-temperature resistivity around the QCP is well expressed by the relation $\rho_m = \rho_0 + A'T^n$. Here ρ_0 is the residual resistivity, A' is a constant, and n is an exponent characteristic to the electronic and magnetic state of the materials. The parameter n is close to 2, 5/3, 3/2, and 1 in a conventional Fermi liquid, a three-dimensional ferromagnet, a three-dimensional antiferromagnet, and a two-dimensional antiferromagnet, respectively.^{31,32} Figure 3(c) displays ρ_0 and n for CePtSi₂ evaluated by fitting the present experimental data between 0.2 and 0.8 K to the above equation as a function of pressure. ρ_0 increases with pressure followed by a maximum around 1.2 GPa indicating an enhancement of Kondo fluctuation. The value of n is 2 at ambient pressure, and it decreases with increasing pressure and closes to 1 around 1.2 GPa, suggesting that the antiferromagnetism in CePtSi₂ has a two-dimensional interaction rather than a three-dimensional one. Above 1.2 GPa, n increases and becomes 1.6 at 2.6 GPa indicating the recovery of the Fermi-liquid state. The minimum of n and maximum of ρ_0 show that a QCP of AF phase of CePtSi₂ exists around 1.2 GPa. The QCP is close to P_{c1} as shown in Fig. 3(a) and smaller than the 2 GPa predicted from the initial slope of T_N vs pressure ($dT_N/dP = -1$ K/GPa). The pressure dependence of T_N is speculated as the dashed line shown in Fig. 3(a).

According to the magnetic interactions model,³¹ the magnetic ordering temperature T_N collapses owing to quantum fluctuation and is proportional to $|P - P_c|^x$, where $x = 2/3$ and 1 for a three- and two-dimensional antiferromagnet, respectively.^{2,33} Indeed, T_N shows linear decrease up to 0.79 GPa as shown in Fig. 3(a). Linear extrapolation of the pressure dependence of T_N , which is based on this model for the

two-dimensional AF, is shown in Fig. 3(a) as a dash-dotted line. That crosses the P axis around P_{c2} indicating that the antiferromagnetism predicted by linear-pressure dependence is suppressed by evolving the superconducting phase.

Note that the superconducting phase appears above P_V , which is consistent with the QCP of the AF phase, as shown in Figs. 3(a) and 3(b). Similar type of superconductivity is observed in $\text{CeCu}_2(\text{Ge},\text{Si})_2$,^{34–37} CeNiGe_3 ,³⁸ and $\text{Ce}_2\text{Ni}_3\text{Ge}_2$,³⁹ in which the superconducting phase appears around the P_V . Jaccard *et al.*³⁴ reported that the merging of T_1 and T_2 indicates an entrance in an intermediate valence state of Ce, while the T_K is of the order of the CEF splitting and Miyake *et al.*^{40–42} have pointed recently the possibility of Ce-based superconductivity due to the valence fluctuation. In CePtSi_2 , the crossover from the concentrated Kondo state to an intermediate valence state is suggested from the change in the magnetoresistance⁴³ and resistivity⁴⁴ around P_V . This intermediate valence state would further disturb the AF phase predicted by linear-pressure dependence around the P_V . Judging from these results, we propose that the AF phase collapsed by magnetic-nonmagnetic quantum fluctuation is further suppressed by the valence fluctuation of Ce, and superconductivity arises in CePtSi_2 .

In summary, the resistivity, magnetoresistance and ac susceptibility of a polycrystalline sample of an orthorhombic

concentrated Kondo compound CePtSi_2 was measured under hydrostatic pressure. T_N decreases with increasing pressure and the QCP exists around 1.2 GPa. The superconducting phase appears between 1.4 and 2.4 GPa with the maximum T_c of 0.14 K at 1.7 GPa. Magnetoresistance measurement indicates that H_{c2} is 0.7 T at 1.7 GPa and is clearly larger than the Pauli limit predicted by the BCS theory. Non-Fermi-liquid behavior was observed around the QCP, and n , the power of temperature dependence of resistivity, was evaluated to be ~ 1 . T_1 and T_2 , the modified Kondo temperatures, merge into a single T_{max} around 1.2 GPa which is consistent with the QCP. These results indicate that a superconductivity in CePtSi_2 is induced at high temperature owing to the quantum instability of the possible two-dimensional AF phase and the valence fluctuation of Ce.

The authors would like to thank T. Komatsubara for the preparation of the sample, and M. Hedo and Y. Saiga for their help in the dilution measurement. They also thank E. V. Sampathkumaran for helpful comments. The crystal structure shown in Fig. 1 was drawn with VENUS developed by Dilanian and Izumi. This work was partially supported by MEXT, the Grant-in-Aid for Scientific Research (Grant No. 20900131).

-
- ¹S. S. Saxena *et al.*, Nature (London) **406**, 587 (2000).
²N. D. Mathur *et al.*, Nature (London) **394**, 39 (1998).
³D. Jaccard *et al.*, Phys. Lett. A **163**, 475 (1992).
⁴H. Hegger *et al.*, Phys. Rev. Lett. **84**, 4986 (2000).
⁵L. Balicas *et al.*, Phys. Rev. Lett. **87**, 067002 (2001).
⁶S. Nakatsuji *et al.*, Nat. Phys. **4**, 603 (2008).
⁷E. D. Bauer *et al.*, Phys. Rev. Lett. **94**, 047001 (2005).
⁸N. Kimura *et al.*, Phys. Rev. Lett. **95**, 247004 (2005).
⁹T. Mito *et al.*, Phys. Rev. Lett. **90**, 077004 (2003).
¹⁰M. S. Torikachvili *et al.*, Phys. Rev. Lett. **101**, 057006 (2008).
¹¹P. Gegenwart *et al.*, Nat. Phys. **4**, 186 (2008).
¹²J. S. Zhou *et al.*, Phys. Rev. Lett. **94**, 226602 (2005).
¹³J. Sichelschmidt *et al.*, Phys. Rev. Lett. **91**, 156401 (2003).
¹⁴S. Sachdev, Science **288**, 475 (2000).
¹⁵E. D. Bauer *et al.*, Phys. Rev. Lett. **94**, 046401 (2005).
¹⁶Y. Tabata *et al.*, Phys. Rev. Lett. **86**, 524 (2001).
¹⁷G. R. Stewart, Rev. Mod. Phys. **78**, 743 (2006).
¹⁸S. Doniach, in *Valence Instabilities and Related Narrow Band Phenomena*, edited by R. D. Parks (Plenum, New York, 1977), p. 169; **91**, 231 (1977).
¹⁹W. H. Lee *et al.*, Phys. Rev. B **42**, 6542 (1990).
²⁰C. Geibel *et al.*, J. Magn. Magn. Mater. **108**, 207 (1992).
²¹J. J. Lu *et al.*, J. Magn. Magn. Mater. **311**, 614 (2007).
²²G. Oomi *et al.*, JJAP Ser. **11**, 165 (1998).
²³T. Nakano *et al.*, J. Phys.: Conf. Ser. **150**, 042139 (2009).
²⁴G. Oomi *et al.*, Physica B **188**, 481 (1993).
²⁵K. Hiebl and P. Rogl, J. Magn. Magn. Mater. **50**, 39 (1985).
²⁶T. Kawai *et al.*, J. Phys. Soc. Jpn. **76**, 014710 (2007).
²⁷Y. Uwatoko *et al.*, Physica B **329**, 1658 (2003).
²⁸A. T. Holmes *et al.*, Phys. Rev. B **69**, 024508 (2004).
²⁹D. Jaccard and A. T. Holmes, Physica B **359**, 333 (2005).
³⁰H. Miyagawa *et al.*, Phys. Rev. B **78**, 064403 (2008).
³¹T. Moriya, *Spin Fluctuations in Itinerant Electron Magnetism* (Springer, Berlin, 1985).
³²T. Moriya and T. Takimoto, J. Phys. Soc. Jpn. **64**, 960 (1995).
³³A. J. Millis, Phys. Rev. B **48**, 7183 (1993).
³⁴D. Jaccard *et al.*, Physica B **261**, 1 (1999).
³⁵B. Bellarbi *et al.*, Phys. Rev. B **30**, 1182 (1984).
³⁶F. Thomas *et al.*, J. Phys.: Condens. Matter **8**, L51 (1996).
³⁷H. Q. Yuan *et al.*, Science **302**, 2104 (2003).
³⁸M. Nakashima *et al.*, J. Phys.: Condens. Matter **16**, L255 (2004).
³⁹M. Nakashima *et al.*, Physica B **378-80**, 402 (2006).
⁴⁰K. Miyake *et al.*, J. Phys. Soc. Jpn. **57**, 722 (1988).
⁴¹A. T. Holmes *et al.*, J. Phys. Soc. Jpn. **76**, 051002 (2007).
⁴²S. Watanabe *et al.*, J. Magn. Magn. Mater. **310**, 841 (2007).
⁴³G. Oomi *et al.*, J. Alloys Compd. **207**, 278 (1994).
⁴⁴H. Miyagawa *et al.*, High Press. Res. **26**, 503 (2006).